

# Chitosan/Rice Straw Nanofibers Nanocomposites: Preparation, Mechanical, and Dynamic Thermomechanical Properties

Mohammad L. Hassan,<sup>1,2</sup> Shaimaa M. Fadel,<sup>1</sup> Nahla A. El-Wakil,<sup>1</sup> Kristiina Oksman<sup>3</sup>

<sup>1</sup>Cellulose and Paper Department, National Research Center, Dokki, Cairo, Egypt

<sup>2</sup>Centre of Excellence for Advanced Sciences, Advanced Materials and Nanotechnology Group, National Research Centre, Dokki, Cairo, Egypt

<sup>3</sup>Division of Manufacturing and Design of Wood and Bionanocomposites, Luleå University of Technology, Luleå, Sweden

Received 20 February 2011; accepted 27 November 2011

DOI 10.1002/app.36606

Published online in Wiley Online Library (wileyonlinelibrary.com).

**ABSTRACT:** Nanofibers were isolated from rice straw pulp using ultrahigh friction grinding and high-pressure homogenization. Chitosan nanocomposites were prepared using the isolated nanofibers at fiber loading from 2.5 to 20% by solution casting and evaporation technique. The effect of nanofiber loading on dry and wet tensile strength, dynamic mechanical thermal properties, and crystallinity of chitosan were studied using tensile testing, thermogravimetric analysis, dynamic mechanical thermal analysis, and X-ray diffraction. Addition of rice straw nanofibers (RSNF) to chitosan resulted in significant improvement in

wet and dry tensile strength, and shift of glass transition temperature ( $T_g$ ) of chitosan matrix to higher values. Chitosan nanocomposites prepared using RSNF (CRSNF) had remarkable wet and dry tensile strength, which could be attributed to presence of both nanofibers and nanosilica particles originally present in rice straw fibers. Addition of RSNF to chitosan did not affect its onset thermal degradation temperature. © 2012 Wiley Periodicals, Inc. *J Appl Polym Sci* 000: 000–000, 2012

**Key words:** rice straw; nanofibers; chitosan; nanocomposites

## INTRODUCTION

Because of the increased awareness of environmental issues regarding the use of biodegradable and natural polymers, researchers in different areas of the world focused their research on the utilization of the huge quantities of agricultural wastes with the aim to produce green materials. For decades, cellulosic fibers isolated from different agricultural wastes have been used in different products such as paper, reconstituted wood, and cellulose derivatives taking into consideration the biodegradability, eco-friendliness, easy availability, sustainability, and light weight of these fibers.

Rice is one of the largest crops in the world. Huge amounts of rice straw remain after harvesting. The problem of effectively cleaning up rice straw mandates proper use and search for new products to avoid the environmental problems posed by such

straws. In some areas in the world, most of the rice straw is burnt by the farmers, and only a small percentage of rice straw is used as animal feed, low quality paper, and particle board. Rice straw fibers have similar properties to hardwood fibers such as short fiber length, hemicelluloses that consist mainly of pentoses (mainly xylose and arabinose sugars), and lignin which consists mainly of syringyl–guaiacyl units.<sup>1</sup> Rice straw fibers are characterized by the presence of high amount of silica (~ 15% of fiber weight). Fiber size and aspect ratio are also important factors for deriving properties. Rice straw fibers have diameters from 5 to 14  $\mu\text{m}$  (average 8  $\mu\text{m}$ ) with lengths from 0.65 to 3.48 mm (average 1.4 mm) giving an average aspect ratio of 170.<sup>2</sup> In addition, rice straw can be biodegraded completely at 50°C within 10 days under static culture.<sup>3</sup>

Because of presence of considerable amount of silica in rice straw, most of research was directed to the use of rice straw fibers in composite materials. For example, rice straw was used in particle board to enhance sound absorption coefficient of composite boards in the middle and high-frequency sound waves<sup>4</sup> Also, rice straw fibers were used as filler in maleated polypropylene,<sup>5</sup> polyvinyl alcohol,<sup>6</sup> waste tires particles,<sup>7</sup> high-density polyethylene,<sup>8,9</sup> low-density polyethylene,<sup>10</sup> and polyester composites.<sup>11</sup>

Correspondence to: M. L. Hassan (mlhassan2004@yahoo.com).

Contract grant sponsors: The funding agency for the collaboration between Luleå University of Technology (Sweden) and National Research Center (Egypt) is SIDA (Swedish International Development Cooperation Agency).

Attention has been paid to cellulose nanofibers derived from agricultural crops–residues due to their huge amounts all over the world and annual renewability especially for countries that do not have forests. Differences in composition and fibers properties (length, diameter, and crystallinity) of the agricultural residues could lead to isolated nanofibers with different properties and therefore nanocomposites with tailored properties. Several studies have been published concerning the use of nanofibers isolated from different lignocellulosic materials as reinforcing elements with different natural and synthetic polymer matrices for different application.<sup>12</sup> Isolation and optimization of nanofibers from rice straw (*Oryza glaberrima*) was first reported by Hassan et al.<sup>13</sup> It is worth mentioning that no work concerning use of rice straw nanofibers (RSNF) as reinforcing elements in biodegradable polymers has been conducted so far.

Chitosan (1,4)-2-amino-2-deoxy- $\beta$ -D-glucan is a naturally occurring polysaccharide polymer composed of glucosamine and *N*-acetyl glucosamine with properties that depend largely on the degree of acetylation, molecular conformation, molecular weight, and its distribution.<sup>14</sup> It finds many applications mainly in biomedical area due to its high resistance toward microbial attack.<sup>15</sup> In such applications, chitosan is used with other organic or inorganic materials to improve its mechanical and dimensional stability in wet conditions.<sup>16–18</sup> Because of its close chemical structure to cellulose, chitosan has been used to prepare composites using cellulose fibers or derivatives as reinforcing elements.<sup>19–22</sup> The transparency of chitosan film containing cellulose fibers or derivatives is greatly reduced. In the area of nanocomposites using chitosan as a matrix and cellulose nanofibers as reinforcing material, few studies have been published so far. In these studies, microfibrillated cellulose isolated from wood pulp, tunicin, and bagasse were used as reinforcing elements and also to enhance wet and dry strength properties of chitosan.<sup>23–26</sup> In addition, modified bacterial cellulose was used as reinforcing filler with chitosan to prepare nanocomposites for medical applications.<sup>27</sup>

Many studies discussed the role of silica in silica-filled nanocomposites to enhance the mechanical properties of polymer matrices.<sup>28,29</sup> However, the effect of natural silica present in rice straw on the physical properties of the nanocomposite has not been studied so far.

The aim of this work is to improve the chitosan film properties by using nanofibers isolated from rice straw pulp to utilize the properties of nanofibers and nanosilica originally present within RSNF. The prepared nanocomposites have expected use in tissue engineering.

## EXPERIMENTAL

### Materials

Unbleached soda rice straw pulp was supplied by Rakta Company for Pulp and Paper, Alexandria, Egypt; the pulp was bleached in the laboratory using sodium chlorite/acetic acid.<sup>30</sup> Chemical composition of the prepared nanofibers was determined according to the standard methods<sup>30</sup> and was found to be  $\alpha$ -cellulose 61.9%, pentosans 22.5%, and ash 16.8% (silica 15.8%). Chitosan powder (high molecular weight grade, degree of deacetylation: 84.7%; viscosity: 200 mPa in 1% acetic acid; relative molar mass: Mr 400,000) was obtained from Sigma-Aldrich.

### High shear ultrafine grinding of the fibers

The pulp was first disintegrated by high-shear mixer using pulp suspensions of 2% consistency. The fibers were then refined using high-shear ultrafine friction grinder or so-called supermasscolloider (MKCA6-2, Masuko Sanguo, Japan) and passed through the instrument up to 30 times. The gap between the discs was adjusted to 9  $\mu$ m.

### Homogenization of the fibers

The refined fibers were homogenized using a two-chamber high-pressure homogenizer (APV-2000, Denmark) after being diluted with water to 1% consistency and passed through the instrument up to 10 times. The pressure was kept at 40 bar in one chamber and 400 bar in the other chamber.

### Preparation of chitosan/cellulose nanofibers nanocomposites

Chitosan was dissolved in 2% acetic acid solution. Mixtures of cellulose nanofibers and chitosan solution were prepared by thoroughly stirring the nanofibers with chitosan overnight. The nanofibers percent in the films is 2.5, 5, 7.5, 10, 15, and 20%. The films were obtained by casting in 15-cm diameter Petri dishes and dried in an oven with circulating air at 35°C for 24 h. The films were removed from the dishes and kept in a relative humidity of 60% at 25°C before testing.

### Characterization of chitosan/cellulose nanofibers nanocomposites

Dry and wet tensile strength properties of the obtained films were measured using a Lloyd universal testing machine at crosshead speed of 5 mm/min using a load cell of 1 kN and 100 N, respectively. The films width was about 1 cm and the gauge length was 4 cm. In wet tensile, the samples were

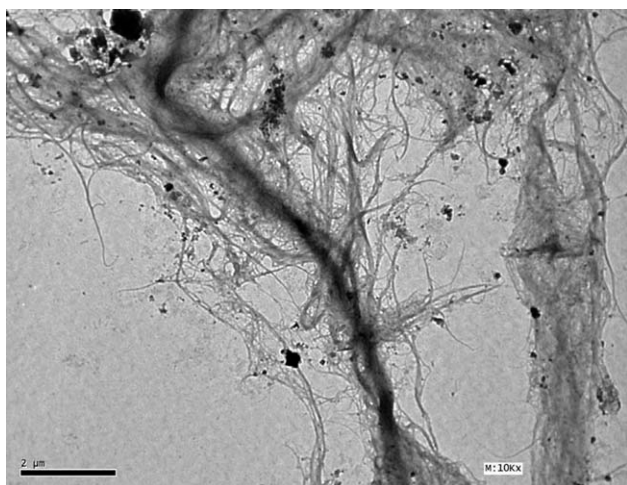


**Figure 1** TEM of nanofibers isolated from rice straw pulp.

immersed in phosphate saline buffer (137 mM NaCl, 2.7 mM KCl, 10 mM sodium phosphate dibasic, 2 mM potassium phosphate monobasic) at pH 7.4 for 24 h before testing.<sup>17</sup> At least five strips from each sample were tested, and the results were averaged. Diffraction patterns were obtained using a Phillips X-ray diffractometer. The diffraction patterns were recorded using Cu-K $\alpha$  radiation at 40 kV and 25 mA. A Perkin-Elmer thermogravimetric analyzer (TGA) was used to study the thermal stability. The heating rate was set at 10°C/min over a temperature range of 50–600°C. Measurements were carried out in nitrogen atmosphere with a flow rate of 50 cm<sup>3</sup>/min. Dynamic mechanical properties were measured using Anton Paar Rheometer, Austria, in tensile mode at a frequency of 1 Hz, strain of 0.1%, and at the heating rate of 3°C/min over the temperature range of –100 to 200°C.

## RESULTS AND DISCUSSION

Nanofibers isolated from rice straw bleached pulp using ultrafine grinding followed by high-pressure homogenization were used with chitosan polymer to prepare cellulosic nanocomposites by solution casting. The diameters of isolated nanofibers were in the range from 4 to 13 nm; even the larger microfibrils had diameter less than 100 nm. Because of the presence of silica in high amounts (~ 15%) in rice straw fibers, the transmission electron microscope (TEM) images of the isolated nanofibers (Fig. 1) showed presence of small particles in the nanoscale; energy-dispersive X-ray (EDX) spectroscopy proved that these nanoparticles are silica.<sup>13</sup> All the prepared nanocomposite films showed homogeneous morphology and good transparency even at high fiber loading due to the size of the nanofibers and nano-silica particles.

### Tensile strength and modulus of chitosan nanocomposites

The effect of loading percent of RSNF on tensile strength and modulus of chitosan/RSNF nanocomposites (CRSNF) was studied, and the results are represented in Figure 2. Remarkable increase in tensile strength took place as a result to addition of RSNF even in case of 2.5% nanofibers loading. The increase in tensile strength could be attributed to formation of percolated/interconnected network of the nanofibers within the chitosan matrix.<sup>31</sup> Although the isolated rice straw and bagasse nanofibers have nearly similar diameters, e.g., 4–13 and 5–15 nm, respectively,<sup>13</sup> the tensile strength of the chitosan nanocomposites loaded with RSNF had more than twice that of the previously studied chitosan nanocomposites loaded with bagasse nanofibers.<sup>32</sup> The increase in tensile strength of chitosan was about 89.6% in case of using bagasse nanofibers, whereas it was 183.5 % in case of RSNF. High RSNF loading (20%) resulted in tensile strength value of

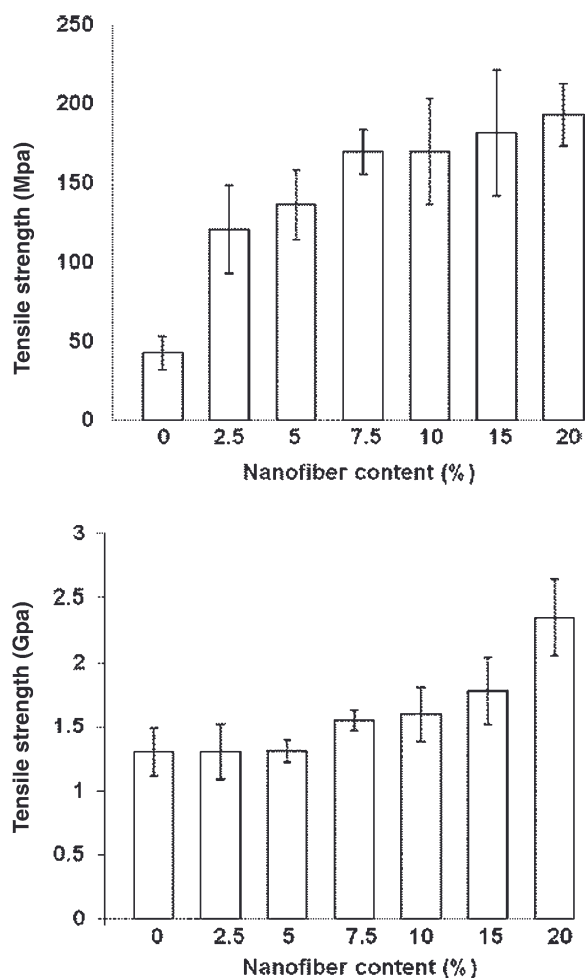


**Figure 2** Tensile strength and tensile modulus of CRSNF nanocomposites.

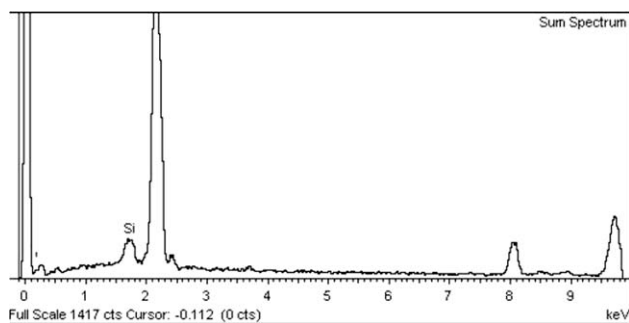


**Figure 3** EDX spectra of chitosan/rice straw nanofibers nanocomposites.

193.2 MPa in the chitosan nanocomposite. This value corresponds to about 355% increase in tensile strength compared to neat chitosan.

Comparing the results of tensile strength of bagasse/chitosan nanocomposites to that of rice straw/chitosan nanocomposites may indicate a role for silica nanoparticles in case of using RSNF, even at low fibers loading. EDX of chitosan nanocomposites films made using RSNF showed presence of silica (Fig. 3). In addition to the major signals of elements of cellulose and chitosan polymers, a significant signal at 1.75 keV, which is attributed to silicon element, appeared in the EDX spectrum of the nanocomposite.<sup>33</sup> The percent of silica present within the nanofibers was about 15%, which means that the percent of silica in the chitosan films ranges from 0.37 to 3% at the different nanofibers loading. However, more evidences are required to support that the reinforcing effect of silica at that low concentration on the properties of chitosane nanocomposites. No published work has been conducted on the nature of interaction between silica and chitosan in the form of quaternary acetic acid salt and the possible mechanism for enhancement of the tensile properties of chitosan. In a previous work of Lee et al.,<sup>17</sup> it was found that silica, which was *in situ* prepared by condensation of tetramethylorthosilane in chitosan-HCl solution, could improve both dry and wet tensile properties of chitosan.

Regarding the tensile modulus of the nanocomposites, no improvement in tensile modulus was observed below 5% nanofibers loading although the tensile strength of chitosan films increased gradually on addition of the nanofibers. This could be attributed to close values of tensile modulus of neat chitosan film and that of RSNF (tensile modulus of 1.25 Gpa for a sheet made from neat RSNF). The increase in tensile modulus of chitosan at 20% nanofibers loading was about 81%. The increase in tensile modulus above the threshold nanofiber loading (>5%) could be attributed to the formation of percolated/interconnected network of the nanofibers within the chitosan matrix.<sup>31</sup>

### Wet tensile strength of chitosan nanocomposites

The effect of loading chitosan with RSNF on wet tensile strength was studied, and the results are presented in Figure 4. It was noticed that films made from neat chitosan suffered from large increase in width due to swelling in the buffer solution before the test, whereas the increase in width for CRSNF was limited even at 2.5% loading. This means that the nanofibers restricted the deformation of the film associated with exposure to water. This property is an important requirement for materials used in tissue engineering where wet conditions play an important role in dimensional stability. The significant improvement of wet tensile strength and dimensional stability of chitosan due to addition of cellulose microfibrils was reported before and was attributed to the formation of percolated/interconnected network of the nanofiber.<sup>32</sup> In addition, formation of crosslinking reaction between chitosan and the trace amount of carbonyl groups exist in cellulose has been reported.<sup>25</sup> From the figure, it is clear that a pronounced increase in the tensile strength starts from 7.5% fibers loading and further increase does not result in significant effect on the tensile strength. In addition, wet tensile strength of CRSNF nanocomposites was higher than that reported previously in case of using bagasse nanofibers.<sup>32</sup>

### Crystallinity of chitosan nanocomposites

The effect of nanofibers loading on crystallinity of chitosan was studied, and the results are presented in Figure 5. Both cellulose and chitosan are semi-crystalline polymers having nearly the same diffraction patterns. When chitosan is dissolved in acetic acid and cast into film, the formed film is highly amorphous. The effect of addition of RSNF on the crystallinity of chitosan matrix was studied by X-ray diffraction (XRD). RSNF showed the known XRD pattern of cellulose I, namely, peaks at  $2\theta$  angles at about 16 and 23, due to reflections from 110 and

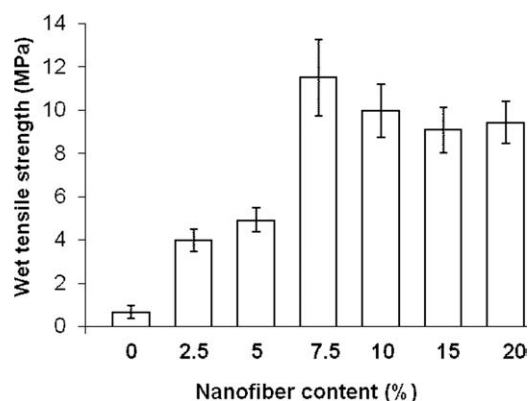


**Figure 4** Wet tensile strength of CRSNF nanocomposites.

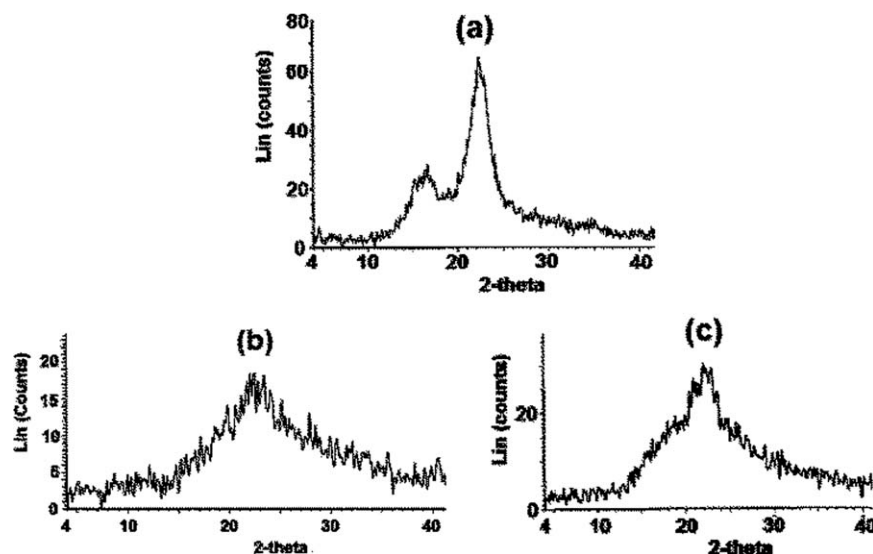


**Figure 5** XRD of (a) rice straw nanofibers, (b) chitosan, and (c) chitosan nanocomposites with 10% rice straw nanofibers.

110 and 020 lattice planes, respectively.<sup>34</sup> Crystallinity index calculated from the diffraction patterns of nanofibers isolated from rice straw was 0.73. The relatively low crystallinity index of the prepared nanofibers could be attributed to presence of amorphous silica which also has broad diffraction peak at  $2\theta$  values close to that of cellulose.<sup>35</sup>

Chitosan films prepared by dissolution in dilute acetic acid and regeneration with alkali usually had three reflections peaks<sup>36</sup> at  $2\theta$  angle of about 21, 19, and 12. In this study, the as-cast chitosan film prepared from chitosan/acetic acid solution, exhibited very broad diffraction pattern with a low-intensity peak at  $2\theta$  angle of about 22 due to the high amorphous nature. The chitosan nanocomposites exhibited diffraction patterns showing the amorphous nature of the prepared nanocomposites with peaks corresponding to both cellulose and chitosan. The peaks in the  $2\theta$  angle range from 23 to 16, which include the peaks of chitosan and cellulose, were overlapped with each other and made it difficult to estimate the crystallinity of chitosan as a result of adding the nanofibers. CRSNF nanocomposites diffraction patterns were similar to that of neat chitosan. This means that the improvement in tensile strength of chitosan as a result of addition of RSNF is not due to increasing the ordering of chitosan chains but could be mainly due to the formation of three-dimensional network of the nanofibers within the chitosan, the possible bonding between chitosan and the few carbonyl groups in the cellulose chain, and interaction between silica nanoparticles and chitosan.

#### Dynamic mechanical thermal properties of chitosan nanocomposites

The effect of nanofibers loading on dynamic mechanical thermal properties of chitosan nanocom-

posites was studied using dynamic mechanical thermal analysis (DMTA) and the DMTA curves are presented in Figure 6. Neat chitosan showed a significant decrease in storage modulus due to relaxation processes with peaks at about 10 and 155°C. When the first decrease in storage modulus started at about -60°C and reached its maximum value at about 10°C, then the modulus increased again. The first decrease in storage modulus at -60°C could be recognized as  $\beta$  relaxation associated with local

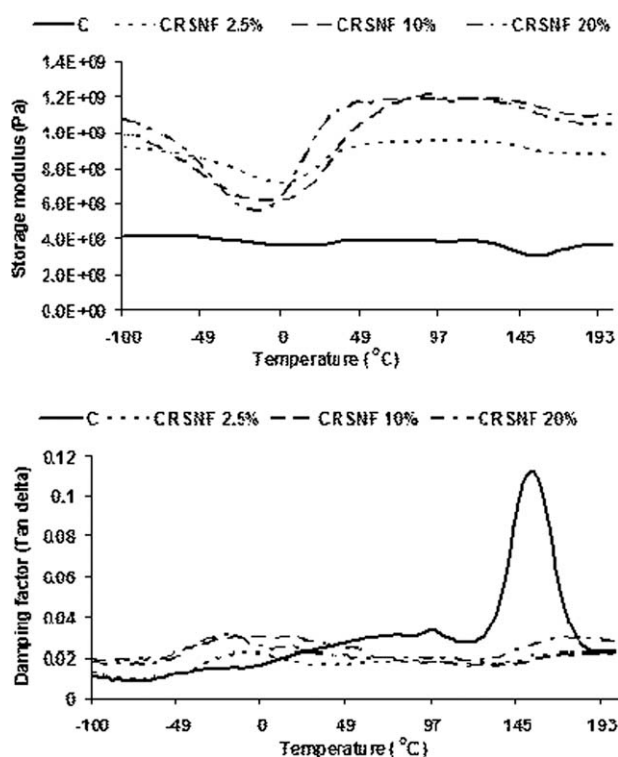


**Figure 6** DMTA of chitosan (C) and CRSNF loaded with 2.5, 10, and 20% rice straw nanofibers.

motion of side groups in chitosan.<sup>36</sup> At temperature higher than freezing temperature of water, structural reorganization of packing of chitosan molecules due to an increase of residual water mobility, volume expansion, and change in hydrogen bond strength took place. Thus, an increase in storage modulus was observed and reached its maximum value at about 45°C.<sup>36</sup> Tan delta curve of neat chitosan showed peaks in accordance with the change in the storage modulus but the first peak which started at -50°C was very broad. The most pronounced decrease in storage modulus and the strongest tan delta peak were at about 155°C. According to previous studies, the chitosan glass transition ( $T_g$ ) is observed between 156 and 170°C.<sup>37,38</sup>

Presence of nanofibers in chitosan matrix resulted in an increase in the storage modulus, especially at temperature higher than room temperature, and shift of the tan delta peak at 152°C to higher temperature with remarkable decrease in its intensity. Although use of RSNF resulted in an increase of the storage modulus of the nanocomposites the tan delta peak at  $T_g$  was not significantly affected by increasing the nanofibers loading. In addition, the area under the tan delta peak that corresponds to  $T_g$  of chitosan remarkably reduced in case of addition of nanofibers. This reflects much less damping of tensile modulus, i.e., lower tensile loss modulus, at  $T_g$  of chitosan in case of presence of the nanofibers than in case of neat chitosan. The curves also clearly shows the reinforcing effect of the nanofibers and chitosan above its  $T_g$  and the interaction between the nanofibers and chitosan chains, which are in the form of positively charged quaternary acetic acid salt. On the other hand, the decrease of the storage modulus of the  $\beta$  relaxation process at 10°C in case of the different nanocomposites was higher than that occurred in case of neat chitosan. Therefore, the area under the tan delta peak at 10°C was bigger than that of neat chitosan. This means that the motion of the side chains of chitosan was easier in the presence of the nanofibers. The tan delta peak was shifted to about 174–179°C at the different nanofibers loading.

Comparing the results obtained in this study to those obtained in case of using bagasse nanofibers<sup>32</sup> shows higher shift of the tan delta peak at  $T_g$  of chitosan in case of RSNF than in case of using bagasse nanofibers where tan delta peak was shifted to about 169–174°C at the same nanofibers loading. The higher shift in case of using RSNF could be attributed to the presence of silica within RSNF and indicates stronger interaction between chitosan and RSNF/silica than between chitosan and bagasse nanofibers.

### Thermal stability of chitosan nanocomposites

Thermal degradation behavior of nanosized cellulose is different from that of cellulose or microcrystalline

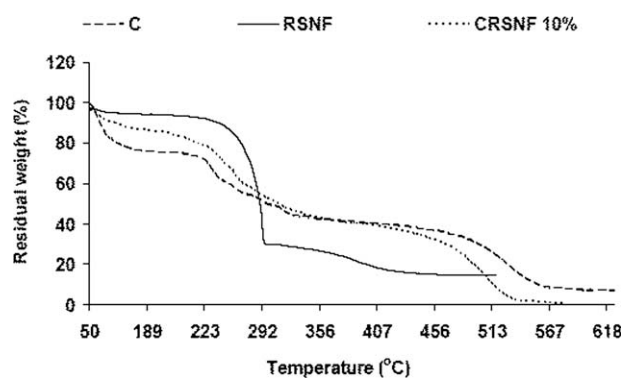


**Figure 7** TGA curves of chitosan (C), RSNF, and CRSNF loaded with 10% nanofibers.

cellulose. This difference is mainly caused by the difference in the particle size. Nanosize cellulose has a great number of chains at the surface due to the small particle size and the high specific surface area. The thermal degradation of cellulose is known to be due to a pyrolytic fragmentation that leads to aromatized entities and finally to a highly crosslinked carbon skeleton. It was reported that thermal degradation of cellulose proceeds via three stages; a first weight loss due to water evaporation, a second weight loss attributed to degradation of cellulose due to evolution of nonflammable gases at about 183–186°C, and a third stage due to degradation and evolution of combustible gases at about 300°C.<sup>39</sup> As shown in Figure 7, RSNF shows onset degradation temperature at 240°C.

On the other hand, the thermal degradation process for chitosan may be a random degradation of chitosan main chains (scission of C—O—C bond) in addition to the detachment of acetyl groups.<sup>40</sup>

The effect of nanofibers loading on thermal stability of CRSNF was studied at 10% nanofibers loading, and the results are presented in Figure 7. The results showed initial loss of water up to about 140°C followed by weight loss due to degradation of cellulose and chitosan polymers at temperature higher than 200°C. RSNF showed onset degradation temperatures at about 240°C and much higher residual weight at 500°C due to presence of silica (~ 15%). Thermal degradation of the neat chitosan film started at lower temperature (~ 220°C) than RSNF probably due to the detachment of the acetyl groups of chitosan during degradation. But the rate of thermal degradation of nanofibers is much faster than chitosan as it is clear from the TG curves and the residual weight at 500°C, which is much higher in case of chitosan. CRSNF had onset degradation temperature and degradation patterns close to that of chitosan. But at temperatures higher than about 430°C, chitosan had lower rate of degradation than the nanocomposites containing nanofibers and higher residual weight at the end of degradation.

## CONCLUSIONS

Chitosan nanocomposites with high wet and dry tensile strength were prepared using nanofibers isolated from rice straw pulp. Presence or RSNF in chitosan affected its dynamic mechanical thermal properties, e.g., glass transition temperature, storage, and loss modulus. Presence of silica, which naturally exists with the rice straw fibers, seems to have an effect on the properties of the chitosan in addition to the main effect of the nanofibers. More evidences are needed to determine the exact role of silica.

## References

- Hans, J. S.; Rowell, J. S. In *Paper and Composites from Agro-Based Resources*; Rowell, M. R.; Young, R. A.; Rowell, J. K., Eds.; CRC Lewis Publishers: New York, 1997; p 83.
- Rials, T. G.; Wolcott, M. P. In *Paper and Composites from Agro-Based Resources*; Rowell, M. R.; Young, R. A.; Rowell, J. K., Eds.; CRC Lewis Publishers: New York, 1997; p 63.
- Wang, W. D.; Cui, Z. J.; Wang, X. F.; Niu, J. L.; Liu, J. B.; Igarashi, Y. *Huan Jing Ke Xue* 2005, 26, 156.
- Yang, H. S.; Kim, D. J.; Kim, H. J. *Biores Technol* 2003, 86, 117.
- Grozdanov, A.; Buzarovska, A.; Bogoeva-Gaceva, G.; Avella, M.; Errico, M. E.; Gentile, G. *INRA EDP Sci* 2006, 26, 251.
- Samir, K. *Polym Adv Technol* 2004, 15, 612.
- Yang, H. S.; Kim, D. J.; Lee, Y. K.; Kim, H. J.; Jeon, J. Y.; Kang, C. W. *Biores Technol* 2004, 95, 61.
- Yao, F.; Wu, Q.; Liu, H.; Lei, Y.; Zhou, D. *J Appl Polym Sci* 2011, 119, 2214.
- Yao, F.; Wu, Q.; Yong, L.; Yanjun, X. *Ind Crop Prod* 2008, 28, 63.
- Habibi, Y.; El-Zawawy, W. K.; Ibrahim, M. M.; Dufresne, A. *Compos Sci Technol* 2008, 68, 1877.
- Hassan, M. L.; Nada, A. M. A. *J App Polym Sci* 2003, 87, 653.
- Plackett, S. *Cellulose* 2010, 17, 459.
- Hassan, M. L.; Mathew, A. P.; Hassan, E. A.; El-Wakil, N. A.; Oksman, K. *Wood Sci Technol*, in press, doi: 10.1007/s00226-010-0373-z.
- Pillai, C. K. S.; Paul, W.; Sharma, C. P. *Prog Polym Sci* 2009, 34, 641.
- Rabea, E. I.; Badawy, M. E. T.; Stevens, C. V.; Smagghe, G.; Steurbaut, W. *Biomacromolecules* 2003, 4, 1457.
- Li, Z.; Ramay, H. R.; Hauch, D. K.; Xiao, D.; Zhang, M. *Biomaterials* 2005, 26, 3919.
- Lee, E. G.; Shin, D. S.; Kim, H. E.; Kim, H. W.; Koh, Y. H.; Jang, J. H. *Biomaterials* 2009, 30, 743.
- Silva, S. S.; Ferreira, R. A. S.; Fu, L.; Carlos, L. D.; Mano, J. F.; Reis, R. L. *J Mater Chem* 2005, 15, 3952.
- Shih, C. M.; Shieh, Y. T.; Twu, Y. K. *Carbohydr Polym* 2009, 78, 169.
- Veerapur, R. S.; Gudasi, K. B.; Aminabhavi, T. M. *J Membr Sci* 2007, 304, 102.
- Lima, I. S.; Lazarin, A. M.; Airoidi, C. *Int J Biol Macromol* 2005, 36, 79.
- Twu, Y. K.; Huang, H. I.; Chang, S. Y.; Wang, S. L. *Carbohydr Polym* 2003, 54, 425.
- Gällstedt, M.; Hedenqvist, M. S. *Carbohydr Polym* 2006, 63, 46.
- Taniguchi, T.; Okamura, K. *Polym Int* 1998, 47, 291.
- Hosokawa, J.; Nishiyama, M.; Yoshihara, K.; Kubo, T.; Terabe, A. *Ind Eng Chem Res* 1991, 30, 788.
- Susana, C. M.; Fernandes, S. C.; Freire, C. S. R.; Silvestre, A. J. D.; Neto, C. P.; Gandini, A.; Berglund, L. A.; Salmén, L. *Carbohydr Polym* 2010, 81, 394.
- Ciechańska, D. *Fibers Text East Eur* 2004, 12, 69.
- Vladimirov, V.; Betchev, C.; Vassiliou, A. G.; Bikiaris, P. *Compos Sci Technol* 2006, 6, 2935.
- Boutaleb, S.; Zaïri, F.; Mesbah, A.; Naït-Abdelaziz, M.; Gloaguen, J. M.; Boukharouba, T.; Lefebvre, J. M. *Int J Solids Struct* 2009, 46, 1716.
- Browning, B. L. In *Methods of Wood Chemistry*; Interscience Publisher: New York, 1967; Chapter 19, p 386.
- Nordqvist, D.; Idermark, J.; Hedenqvist, M. S. *Biomacromolecules* 2007, 8, 2398.
- Hassan, M. L.; Hassan, E. A.; Oksman, K. N. *J Mater Sci* 2010, 46, 1732.
- Kalapathy, U.; Proctor, A.; Shultz, J. *Biores Technol* 2000, 73, 257.
- Wada, M.; Heux, L.; Sugiyama, J. *Biomacromolecules* 2004, 5, 1385.
- Vijayalakshmi, U.; Balamurugan, A.; Rajeswari, S. *Trends Biomater Artif Organs* 2005, 18, 101.
- Tripathi, S.; Mehrotra, G. K.; Dutta, P. K. *Carbohydr Polym* 2010, 79, 711.
- Mucha, M.; Pawlak, A. *Thermochim Acta* 2005, 427, 69.
- Neto, C. G.; Giacometti, J. A.; Job, A. E.; Ferrira, F. C.; Fonseca, J. L.; Pereira, M. R. *Carbohydr Polym* 2005, 62, 97.
- Klemm, D.; Philipp, B.; Heinze, U.; Wagenknecht, W. In *Comprehensive Cellulose Chemistry*; Wiley-VCH: Weinheim, 1998; Vol. 1, p 107.
- Wanjuan, T.; Cunxin, W.; Chen Donghua, C. *Polym Degrad Stab* 2005, 87, 389.